APPLICATION OF RANDOM FINITE ELEMENT METHOD TO BEARING CAPACITY DESIGN OF STRIP FOOTING

Giovanna Vessia[1], Claudio Cherubini[2], Joanna Pieczyńska[3], and Wojciech Puła[4]

ABSTRACT

According to the reliability-based design approach suggested by Eurocode 7, the random finite element method has been employed for calculating the reliability index for the bearing capacity design of strip foundation. Such study has been carried out on a well-defined soil from a stochastic point of view, that is the grey-blue clay from Taranto area. The RFEM formulation used has been implemented by Griffiths and Fenton but here the authors have focused on a description of the anisotropic random field for c and ϕ design variables. Results clearly show that the introduction of anisotropy in random fields makes RFEM predictions effective for design purpose because it is less conservative and more realistic than the isotropy assumption.

Key words: RFEM, bearing capacity, strip foundation, anisotropic random field.

1. INTRODUCTION

The shallow footing geotechnical design is mainly based on the evaluation of the bearing capacity. Random character of physical and mechanical soil properties heavily influences the randomness of the bearing capacity estimation which is not usually taken into account into practice.

New building codes as Eurocodes and Italian TU 2008 have absorbed the contribution of about 30 year research in random field and nowadays reliability-based design is one of the suggested design approaches. Nonetheless whenever 2D numerical simulations are employed for the estimation of the shallow footing bearing capacity, the random finite element method (RFEM) can be used. Such a numerical methodology was introduced by Griffiths and Fenton (Griffiths and Fenton 1993; Fenton and Griffiths 1993) and employed in many applications (Griffiths and Fenton 2001; Fenton and Griffiths 2003; Griffiths *et al*. 2002; Griffiths and Fenton 2004; Fenton and Griffiths 2005; Griffiths *et al*. 2006). By now over 50 papers applying this methodology in geotechnics have been reported. RFEM connects random field theory (Vanmarcke 1984) and deterministic formulation of the finite element method by taking into account mean value, standard deviation, correlation length of strength and load design parameters. Thus, implementing Terzaghi's formula (Terzaghi 1943) into RFEM the bearing capacity can be calculated as follows:

$$q_f = c\, N_c + \overline{q}\, N_q + \frac{1}{2}\gamma\, BN_\gamma \tag{1}$$

where q_f is the ultimate bearing stress, c is the cohesion, q is the overburden load due to foundation embedment, γ is the soil unit weight, B is the footing width, and N_c, N_q and N_γ are the bearing capacity factors. To simplify the analysis and focus on the random character of soil parameters Eq. (1) is accordingly simplified (neglecting the contributions of both the footing embedment and the soil weight) for the case of drained conditions:

$$q_f = c\, N_c \tag{2}$$

where the N_c expression is given below (Bowles 1996):

$$N_c = \frac{e^{\pi \tan\phi} \tan^2\left(\frac{\pi}{4}+\frac{\phi}{2}\right) - 1}{\tan\phi} \tag{3}$$

In this paper the authors focused their attention on analyzing the influence of some relevant aspects of the random characterization of soil by means of the numerical algorithm created by Fenton and Griffiths (2003), that is:

- the rule of anisotropy in random field approach to soil parameters, implemented by analyzing different values of correlation length along vertical and horizontal direction;
- verification of the worst case, which means that in every single situation it is possible to assign the characteristic value of correlation length corresponding to the most conservative evaluation of the bearing capacity;
- to investigate random variability of soil properties based on statistical data resulting from real soil testing. The soil under investigation is the grey-blue clay from South East of Italy.

2. THE RANDOM FIELD FORMULATION FOR SOIL

The random soil model proposed by Fenton and Griffiths (2003) describes strength soil parameters by means of isotropic two-dimensional random field by local averaging approach (Vanmarcke 1984).

Two random field variables are taken into account in this paper, that is c and ϕ.

Manuscript received September 1, 2009; revised December 16, 2009; accepted December 21, 2009.

[1] Contract researcher (corresponding author), Department of Civil and Environmental Engineering, Technical University of Bari, Via Orabona, 4, Italy (e-mail: g.vessia@poliba.it).

[2] Full professor, Department of Civil and Environmental Engineering, Technical University of Bari, Via Orabona 4, Italy (e-mail: c.cherubini@poliba.it).

[3] Ph.D. student, Wroclaw University of Technology, Wybrzeże Wyspiańskiego 27, Poland (e-mail: joanna.pieczynska@pwr.wroc.pl).

[4] Associate Professor, Wroclaw University of Technology, Wybrzeże Wyspiańskiego 27, Poland (e-mail: Wojciech.Pula@pwr.wroc.pl).

The cohesion random field is assumed to be lognormal distributed with mean μ_c, standard deviation σ_c and different spatial correlation lengths θ_{cy} and θ_{cx} in vertical and horizontal direction, respectively.

Theoretical aspects of the anisotropic random field assumption have been analyzed in earlier papers (Pula and Shahrour 2003; Pula 2004).

Lognormal random field is derived from a normally distributed random field $G_{\ln c}(\mathbf{x})$, having zero mean, unit variance and spatial correlation length $\theta_{\ln c}$ transformed as follows:

$$c(\mathbf{x}) = \exp\left\{\mu_{\ln c} + \sigma_{\ln c} G_{\ln c}(\mathbf{x})\right\} \tag{4}$$

where x is the spatial position at which c is calculated and $\mu_{\ln c}$ and $\sigma_{\ln c}$ parameters are obtained as mean and standard deviation values of cohesion function:

$$\sigma^2_{\ln c} = \ln\left(1 + \frac{\sigma_c^2}{\mu_c^2}\right) \tag{5}$$

$$\mu_{\ln c} = \ln \mu_c - \frac{1}{2}\sigma^2_{\ln c} \tag{6}$$

Such a transformation is very useful because there are many effective methods for generating normal field and then using Monte Carlo simulation. Realizations of cohesion field have been calculated after having generated the realization of normal field using the transformation in Eq. (4). Correlation structure of cohesion lognormal field $G_{\ln c}(\mathbf{x})$ is expressed by determining the correlation function, whose parameters are correlation lengths along the two directions $\theta_{(\ln c)y}$ and $\theta_{(\ln c)x}$.

In this paper the following correlation function has been assumed:

$$\rho_{\ln c} = \exp\left(-\sqrt{\left(\frac{2(\tau_2)}{\theta_{(\ln c)x}}\right)^2 + \left(\frac{2(\tau_1)}{\theta_{(\ln c)y}}\right)^2}\right) \tag{7}$$

where $\tau_1 = y_2 - y_1$ and $\tau_2 = x_2 - x_1$ are the two components of the absolute distance between the two points in 2D space where the correlation function is calculated by taking into account the anisotropic character of the random field ($\theta_{(\ln c)y}$ and $\theta_{(\ln c)}$). It is worth mentioning that such a correlation function works in a normal random field ln c. $\theta_{(\ln c)y}$ and $\theta_{(\ln c)x}$ values are derived from θ_{cy} and θ_{cx} values.

Correlation lengths θ_{cy} and θ_{cx} can be drawn from in situ tests. One method for converting soil testing results into correlation length is the moment method (Baecher and Christian 2003). Such methodology has been used in this paper.

The second random field considered in this paper is the friction angle. Since friction angle values change within a bounded interval, neither normal nor lognormal distributions are appropriate models for random variable. Fenton and Griffiths (2003) represented bounded distributed fields as a bounded distribution which resembles a beta distribution but arises as a simple transformation of a $G_\phi(\mathbf{x})$, according to:

$$\phi(x) = \phi_{\min} + \frac{1}{2}(\phi_{\max} - \phi_{\min})\left\{1 + \tanh\left(\frac{sG_\phi(x)}{2\pi}\right)\right\} \tag{8}$$

where $\phi_{\min}$ and $\phi_{\max}$ are the minimum and maximum values of friction angle, respectively, and s is the scale factor depending on standard deviation.

Shapes shown in Fig. 1 represent probability distribution functions of ϕ variable. In the graph, ϕ functions are reported for three different scale factor values s. For s values greater than 5 frequency distribution leads to a U-shaped function which is unrealistic in current situations. The mean distribution is in the middle of the interval [$\phi_{\min}$, $\phi_{\max}$]. Relationship between the standard deviation and the scale parameter s has no analytic form. It can be obtained by numerical integration or by Taylor's expansion. The first order approximation leads to:

$$\sigma_\phi \approx \frac{1}{2}(\phi_{\max} - \phi_{\min})\frac{2s}{\pi\left(\exp(2\phi_0) + \exp(-2\phi_0) + 2\right)} \tag{9}$$

where ϕ_0 is the mean value of the friction angle. Correlation function and correlation length values have been estimated as in the case of cohesion.

3. THE CASE STUDY OF ITALIAN BLUE-GREY CLAY

In the study that follows, the case of Taranto blue-grey clay from South East of Italy (Fig. 2) has been considered. Such soil was widely described in terms of deterministic and random properties in Cherubini *et al*. (2007).

Taranto clays are stiff overconsolidated clays of mainly illitic and kaolinitic mineralogical composition. Figure 3 shows the stratigraphies corresponding to the 15 performed boreholes which show the presence of two clay horizons: the upper weathered yellow clay and the lower blue-grey clay.

As a matter of fact, this soil is characterized, on a regional scale, by a brownish-yellow upper horizon and a grey lower horizon corresponding to the same grey-blue clay formation. Both clays can vary from clayey silt to silty clay. The vertical strength variability in Taranto clays has been defined by means of statistical treatment of data coming from CPTs. In Table 1 the trend and the scale of fluctuation of the cone bearing profiles along the five boreholes for both the upper (a) and the lower (b) clays are listed.

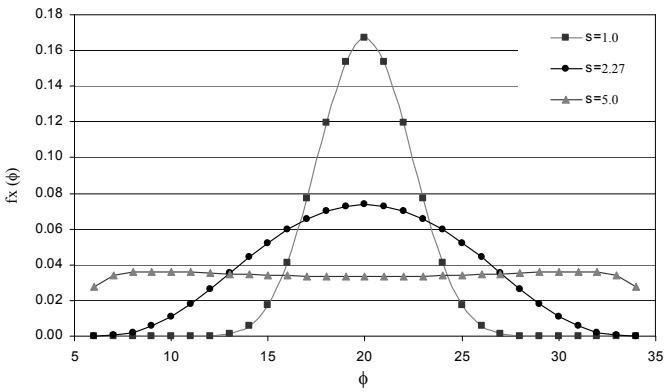

Fig. 1 Shapes of friction angle distribution of bounded type. The curve corresponding to s = 2.27 (σ_ϕ = 4.8°) is the density of the distribution used in this paper for computations

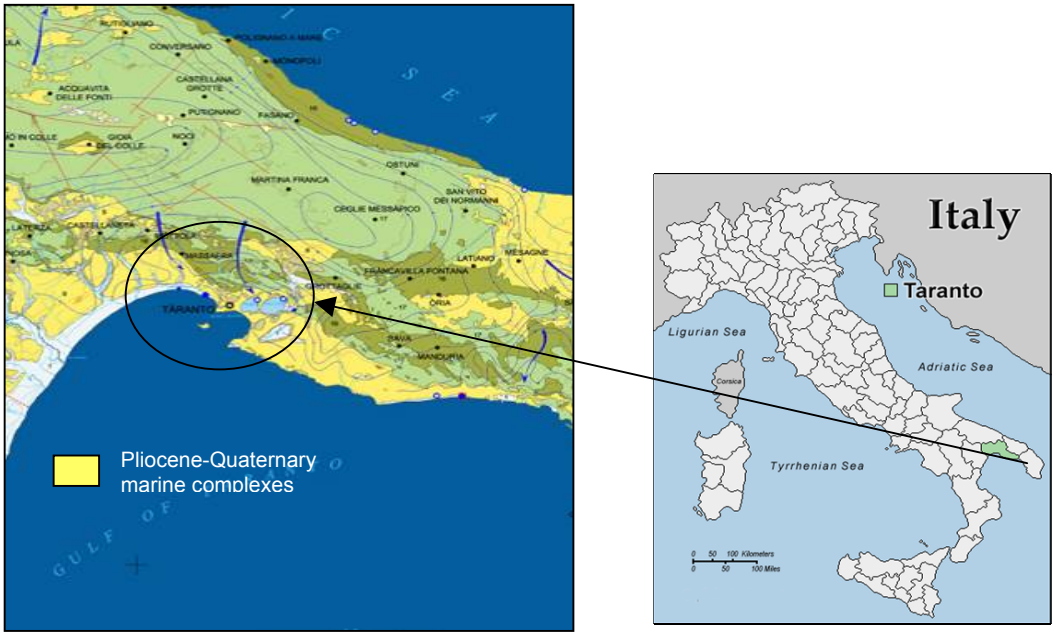

Fig. 2 Geographical set of Taranto grey-blue clay

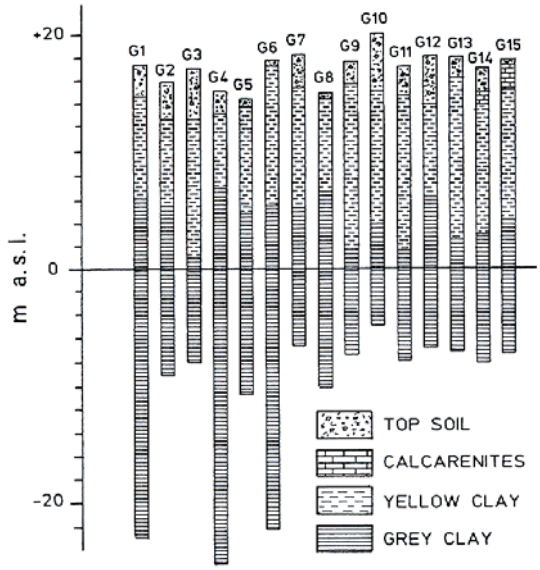

Fig. 3 Stratigraphies from cone penetration testing

The residuals were obtained by removing a low-order polynomial trend, no higher than a quadratic, by regressing the cone bearing values using the ordinary least-square (OLS) method. Furthermore, geostatistical boundaries of the two Taranto clays were investigated by means of intraclass correlation coefficient RI (Wickremesinghe and Campanella 1991).

Figure 4 shows an example of RI profiles coming from processing the q_c, f_s profiles along G1. Results from other profiles confirm the lithological boundary at about 11 m. The whole random field characterization has been synthesized in Table 2.

The mean cohesion $\mu_c = 36$ kPa and standard deviation cohesion $\sigma_c = 20$ kPa have been kept constant, while the friction angle has been defined as being bounded distributed with lower limit $\phi_{min} = 5°$, upper limit $\phi_{max} = 35°$, mean value $\mu_\phi = 20°$, standard deviation $\sigma_\phi = 4.8°$ and scale parameter $s = 2.27$.

Table 1 Trend and scale of fluctuation from CPT within upper and lower clay

Cone penetration	Trend	Scale of fluctuation (m)
Upper clay		
G1	$y = 54.671 \times 2 - 21.21x + 5301$	0.195
G3	$y = 12.44 \times 2 + 113.06x + 2950$	0.401
G6	$y = 40.713 \times 2 - 439.7x + 5601$	0.207
G7	$y = 73.690 \times 2 - 172.2x + 9753$	0.401
G15	$y = 11.027 \times 2 + 212.3x + 2541$	0.436
Lower clay		
G1	$y = 149.11x + 4732$	0.536
G3	$y = 319.58x + 1722$	0.287
G6	$y = 201.29x + 3700$	0.720
G7	$y = 201.14x + 4036$	0.269
G15	$y = 203.34x + 3699$	0.185

4. RANDOM FINITE ELEMENT METHOD

The bearing capacity analysis carried out in this paper uses an elastic perfectly plastic stress strain law with a classical Mohr Coulomb failure criterion according to Fenton and Griffiths (2003) work. Plastic stress redistribution is accomplished using a viscoplastic algorithm. The program uses 8 node quadrilateral elements and reduced integration in both the stiffness and stress redistribution parts of the algorithm. The theoretical basis of the method is described in detail in Chapter 6 of the text by Smith and Griffiths (1998). The finite element model incorporates five parameters: Young's modulus (E), Poisson's ratio (ν), dilation angle (ψ), shear strength (c), and friction angle (ϕ). In the present study E, ν and ψ are held constant (at 910 MPa, 0.3, and 0, respectively) while c and ϕ are randomized. Setting the dilation angle to zero means that there is no plastic dilation during yield of the soil. This is the case in the following computations. The

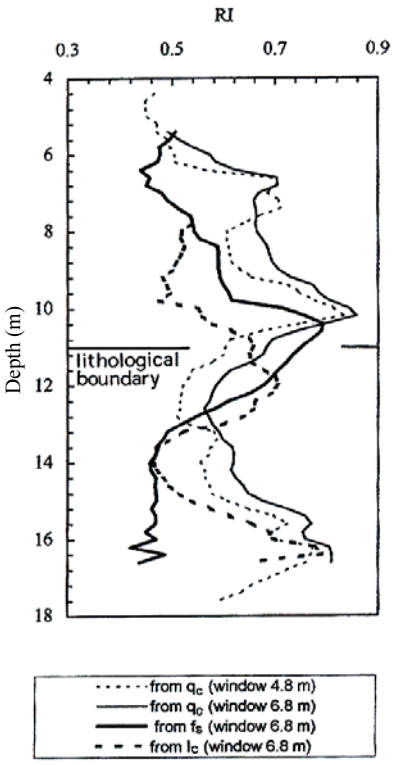

Fig. 4 Intraclass correlation coefficient profiles of cone bearing, sleeve friction and soil behaviour index along G1 in situ CPT test

Table 2 Random mechanical characterization of grey-blue clay

Variable	Probability distribution	Mean μ	Standard deviation σ	Scale of fluctuation θ
c	Lognormal	36 kPa	20 kPa	0.2, 0.3, 0.5, 0.7 m
ϕ	Bounded (see Eq. (8))	20°	min 5° max 35°	0.2, 0.3, 0.5, 0.7 m
γ	Constant	19 kN/m^3	–	–

Young's modulus governs the initial elastic response of the soil, but does not affect the bearing capacity. Thus such elastic soil parameter has been used for pre-analyzing the system. The finite element mesh consists of 1000 elements, 50 elements wide by 20 elements deep (Fig. 5).

Each element is a square of side length 0.1 m and the strip footing occupies 10 elements, thus giving a width of B = 1 m. Since the depth of the model is only 2B some boundary effect can appear. In order to check the correctness of the mesh model an analysis of the mesh influence on the bearing capacity mean value has been carried out. The results are shown in Appendix 1. The random fields in this study are generated using the Local Average Subdivision (LAS) method (Fenton and Vanmarcke 1990). Cross-correlation between the two soil property fields (c and ϕ) is neglected in the present study (see Appendix 2). Numerical analyses of the bearing capacity have been carried out according to the following steps:

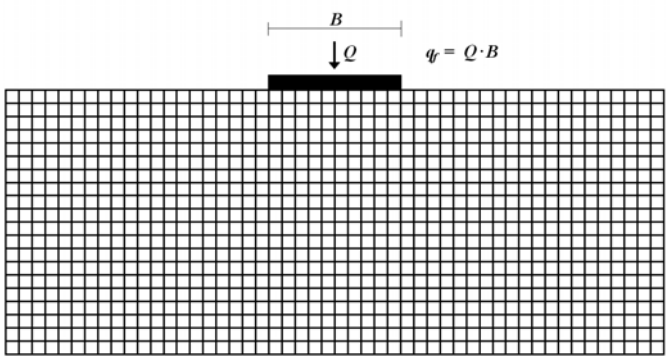

Fig. 5 Mesh model used in stochastic bearing capacity predictions (After Griffiths and Fenton 2001)

1. At first, the accuracy of the calculation of the first two moments (mean and variance) of the bearing capacity has been assessed. Thus numerical simulations by means of Monte Carlo method were made with a variable number of realizations. Results for 300, 500 and 1000 realizations are reported in Fig. 6. There, the confidence intervals considered with selected exceeding probability α = 0.05 are as follows: lower bound of mean value: 450.22 kPa, upper bound of mean value: 481.00 kPa; lower bound of standard deviation: 164.67 kPa, upper bound of standard deviation: 186.46 kPa. Accordingly the optimum number of realizations turned out to be 300; whereas more than 1000 realizations are needed to determine the approximate form of the bearing capacity distribution.
2. At second, the bearing capacity of the system has been calculated for an isotropic case selecting 7 values of fluctuation scale. The values 0.2, 0.3, 0.5, 0.7 m have been reported in the soil testing described in Table 2. Values 1.0, 1.5, 2.0 m have been considered only to catch a trend in the results obtained. According to the assumptions listed in paragraph 3, the correlation lengths of cohesion and friction angle were taken equal. Results from numerical computations are reported in Table 3.

   The results are also presented graphically in Figs. 7 and 8. It is important to point out that the initial value of the correlation length 0.2 m is comparable with the size of the single element of the mesh (0.1 m). This implies strong averaging of random field fluctuations. As a consequence we may expect inaccuracy with the bearing capacity value in this case. However, the average value, as well as the coefficient of variation of the bearing capacity corresponding to 0.2 m of the correlation length, fit well in with the trend obtained from other results. The isotropic case under consideration ($\theta_y / B = \theta_x / B$) has shown the so-called "worst case" for mean value. Figure 7 shows the value of normalized fluctuation scale equal to 1 by which the minimal value of bearing capacity appears. Such outcome is in accordance with the observations made in papers by Griffiths and Fenton (2001) and Fenton and Griffiths (2003).

   The presence of such minimum value is recognized to be an important information, which allows to determine the "true value" of correlation length even when not enough measurements

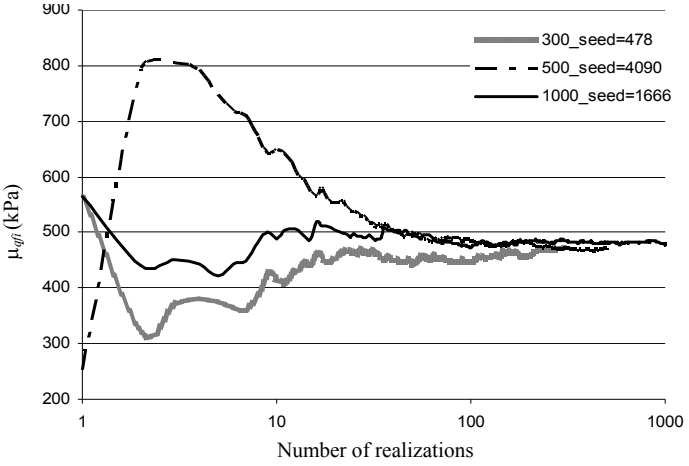

Fig. 6 Testing of convergence rate for mean value of bearing capacity. Runs have been started from three different seeds

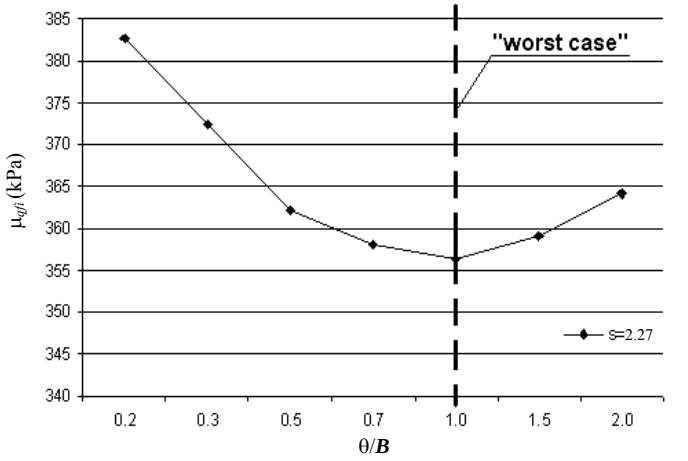

Fig. 7 Mean value of bearing capacity versus normalised fluctuation scale. The parameter *s* is the scale parameter of friction angle distribution. The value *s* = 2.27 corresponds to σ_ϕ = 4.8° assumed for the computations

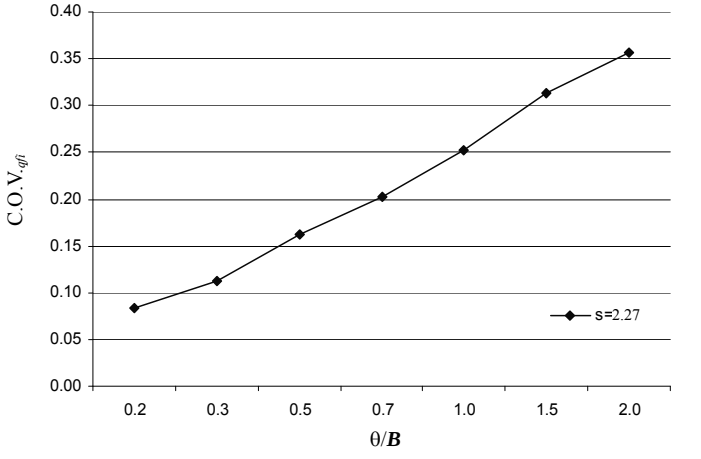

Fig. 8 Coefficient of variation of bearing capacity versus normalised fluctuation scale

Table 3 Mean values, standard deviations and variation coefficients of bearing capacity resulting from isotropic case

θ_x (m)	θ_y (m)	μ_{afi} (kPa)	σ_{afi} (kPa)	C.O.V.$_{qfi}$	Reliability index β
0.2	0.2	382.63	31.67	0.083	7.8
0.3	0.3	372.37	41.97	0.113	5.5
0.5	0.5	362.09	58.72	0.162	3.6
0.7	0.7	357.99	72.51	0.203	2.8
1.0	1.0	356.40	89.80	0.252	2.2
1.5	1.5	359.10	112.67	0.314	1.7
2.0	2.0	364.07	129.69	0.356	1.6

from soil testing are available. Such an approach has a drawback, that is the random bearing capacity predictions are prevalently influenced by standard deviation and bearing capacity coefficient of variation. As standard deviation of bearing capacity and its coefficient of variation are concerned both curves increase with the ratio θ_y/B (Fig. 8).

It means there are no any local minima, which can be considered as the "worst case". It is interesting to highlight that the minimum value of the mean bearing capacity has been accomplished when the ratio θ/B equals one. It is worth mentioning, however, that the value θ = 1.0 has been added "artificially" in this study, because it has not been observed in the soil testing described in paragraph 3.

3. As third step, computations for anisotropic case $\theta_y/B \neq \theta_x/B$ have been carried out. The cases investigated are obtained by changing the correlation lengths in both horizontal and vertical directions. In vertical direction, four values of correlation length θ_y have been considered: 0.2, 0.3, 0.5, 0.7 m and additionally 1.0, 1.5 and 2.0 m.

In horizontal direction, five values of θ_x have been investigated 1, 5, 10, 30, 50 m. As in the previous case, the correlation lengths of cohesion and friction angle were taken as equal. Results are shown in Table 4. And graphically presented in Figs. 9, 10 and 11.

It is easy to notice from Table 4 that the coefficient of variation of friction angle strongly affects standard deviation value and bearing capacity coefficient of variation. Standard deviation raises as the vertical correlation length increases as a matter of fact when correlation length increases the trend in mean and standard deviation of bearing capacity gets flatter. One can observe that the effect of horizontal fluctuation scale is important. However for larger values, which are realistic in natural soils, the bearing capacity coefficient of variations seem to be not very sensitive to the increase in the horizontal scale value. This result can be valuable if we are not able to precisely determine the horizontal fluctuation scale. Moreover, from Fig. 9 another relevant difference between isotropic and anisotropic case can be figured out: the worst case in isotropic case falls constantly at θ_y/B = 1. Such outcome is not true in the anisotropic case: It changes according to θ_x values in θ_y/B range between 0.3 and 0.5. These values cannot be predicted in advance and are more frequently calculated for natural soils with respect to the one in isotropic case.

Table 4 Mean values, standard deviations and coefficients of variation obtained in anisotropic case

	θ_x	θ_y (m)						
	(m)	0.2	0.3	0.5	0.7	1.0	1.5	2.0
μ_{qfi} (kPa)	1	361.97	355.58	351.86	352.73	356.40	363.30	369.12
σ_{qfi} (kPa)		52.70	60.88	72.33	80.77	89.80	100.08	106.72
C.O.V.$_{qfi}$		0.15	0.17	0.21	0.23	0.25	0.28	0.29
Reliability index β		4.0	3.3	2.7	2.4	2.2	2.1	2.0
μ_{qfi} (kPa)	5	369.76	365.01	362.44	363.28	366.99	372.31	376.46
σ_{qfi} (kPa)		77.01	90.15	109.25	123.31	138.28	154.50	164.21
C.O.V.$_{qfi}$		0.21	0.25	0.30	0.34	0.38	0.41	0.44
Reliability index β		2.9	2.4	1.9	1.6	1.5	1.4	1.3
μ_{qfi} (kPa)	10	376.99	373.87	373.69	376.67	381.80	391.07	397.71
σ_{qfi} (kPa)		83.04	97.19	118.21	134.69	153.96	179.26	194.88
C.O.V.$_{qfi}$		0.22	0.26	0.32	0.36	0.40	0.46	0.49
Reliability index β		2.8	2.3	1.9	1.7	1.5	1.3	1.3
μ_{qfi} (kPa)	30	384.71	383.30	386.19	391.55	399.76	411.18	420.42
σ_{qfi} (kPa)		86.99	101.77	123.58	140.72	160.46	185.61	206.07
C.O.V.$_{qfi}$		0.23	0.27	0.32	0.36	0.40	0.45	0.49
Reliability index β		2.8	2.4	1.9	1.8	1.6	1.5	1.4
μ_{qfi} (kPa)	50	386.59	385.80	389.63	395.59	404.68	417.64	428.23
σ_{qfi} (kPa)		88.08	103.20	125.31	142.25	162.29	186.21	206.77
C.O.V.$_{qfi}$		0.23	0.27	0.32	0.36	0.40	0.45	0.48
Reliability index β		2.8	2.4	2.0	1.8	1.6	1.5	1.4

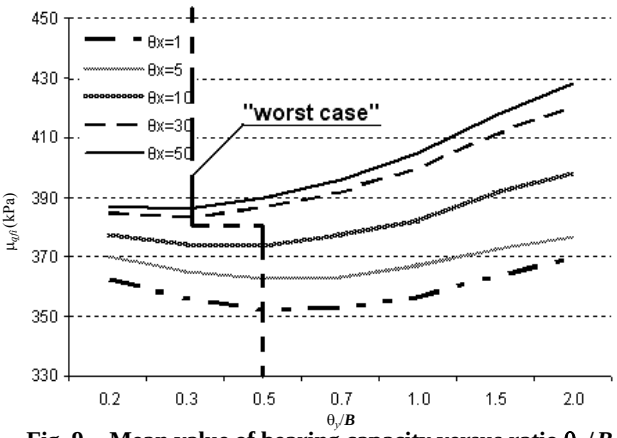

Fig. 9 Mean value of bearing capacity versus ratio θ_y / B for different values of horizontal fluctuation scale

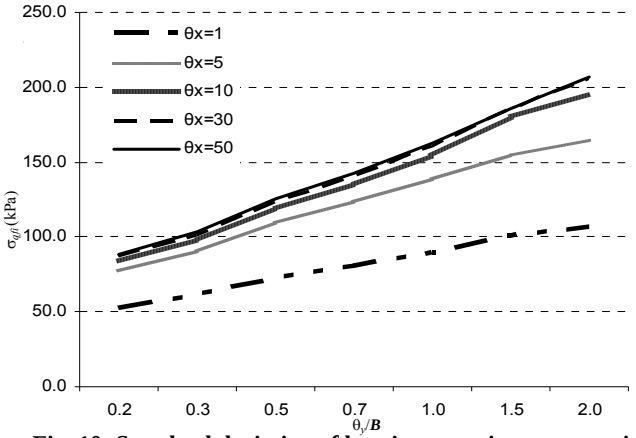

Fig. 10 Standard deviation of bearing capacity versus ratio θ_y / B for different values of horizontal fluctuation scale

5. PROBABILITY DISTRIBUTION OF BEARING CAPACITY

Finally, the probability distribution of the bearing capacity in grey-blue clay has been estimated in order to have enough information for applying reliability-based design approach. Log-normal charts and Komogorov-Smirnov, Chi-square distribution and Anderson-Darling tests have been used to this end.

Here statistics for performing the above mentioned tests are reported according to 2000 realizations just for the case of 30 m

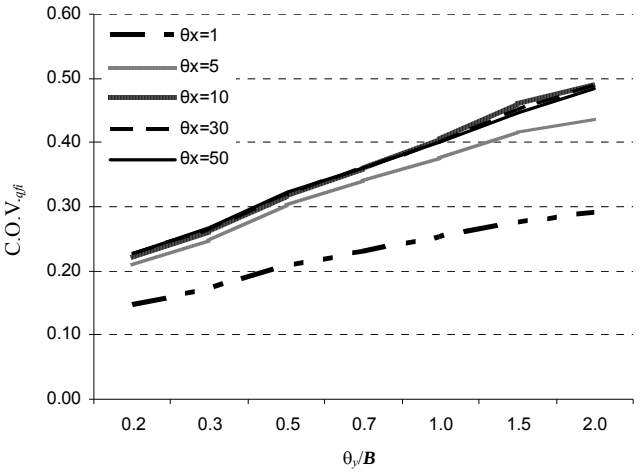

Fig. 11 Coefficient of variation of bearing capacity versus ratio θ_y/B for different values of horizontal fluctuation scale

horizontal and 0.7 m vertical scale of fluctuation (Table 5) whereas Fig. 12 show results of the Lognormal chart according to the numerical values summarized in Table 6.

Figures 13 and 14 show the cumulative distribution function and the density probability distribution of the tested bearing capacity data.

Such results agree with the ones demonstrated by Griffiths and Fenton (2003). In order to show the direct usage of RFEM results in reliability-based design of the strip foundation the lognormal distribution of bearing capacity is here used. Accordingly, the probability value associated with the safety margin can be calculated as follows:

$$P\,[SM<0]=\Phi\left(\frac{\ln\,(Q_d)-\mu_{\ln(q_{fin})}}{\sigma_{\ln(q_{fin})}}\right) \tag{10}$$

where the safety margin SM = Load-Resistance = $Q_d - q_{fin}$: Q_d is the stress design value from the upper structure analysis and q_{fin} is the bearing capacity of the strip foundation. According to Cornell definition of reliability index β, the expression on the right hand side of Eq. (10) can be assumed equal to −β. Thus, let us consider a value of Q_d = 200 kPa for the case of a three-storey building with foundation width B = 3 m, then β has been calculated in Tables 3 and 4 according to the ratio in Eq. (10). Comparing results from isotropic and anisotropic random field characterization (Fig. 15) three main elements can be pointed out:

1. Reliability index β decreases when fluctuation scales along x and y directions increase: Differences can be seen in β values which are less conservative in the isotropic case.
2. Isotropic case is much more sensitive to the increases in the scale of fluctuation than anisotropic case: as a matter of fact, when the field is anisotropic all the cases considered give quite the same β values as θ_y increases and the reduction in β values is about 2 units. Conversely, for the isotropic field as θ_y varies from 0.2 to 2.0 β values reduce from about 8 to less than 2.
3. In anisotropic case β values is more influenced by standard deviation than by θ_x values. Accordingly, in Fig. 15, β values for θ_x = 50 are higher than β values for θ_x = 5 although such differences are negligible. It also means that when θ_x gets much higher than θ_y (from double to two orders of magnitude) its influence on β values becomes negligible with respect to θ_y.

Such outcomes show the ability of RFEM method to be applied directly to strip foundation design but anisotropic random field shall be considered because the isotropic simplification is neither conservative nor realistic.

Table 5 Bearing capacity main statistics

Minimum (kPa)	78.35
Maximum (kPa)	995.6
Range (kPa)	917.25
Median (kPa)	361.1
Arithmetic mean (kPa)	385.32
Geometric mean (kPa)	361.67
Mean square (kPa)	19356
Variance	19366
Stand. Deviation (kPa)	139.16
Coef. of variation	0.36116
Third moment	2.48E+06
Stand. skewness	0.92249
Fourth moment	1.57E+09
Stand. kurtosis	4.201
Variance of mean	9.6782
Var. of variance	1.24E+15
Var. of 3. moment	8.03E+10
Var. of 4. moment	3.08E+16

Table 6 Tests for the estimation of the bearing capacity probability distribution

	Parameter estimation for the case of 30 m horizontal and 0.7 m vertical scale of fluctuation	
Selected estimation method	Method of moments	Least square
Selected stochastic model	Lognormal (3)	
Parameter 1 [xi]	362.405	361.667
Parameter 2 [delta]	0.350151	0.360266
	Testing	
Selected testing method	Kolmogorov-Smirnov test	
Significance level	0.62055	0.79883
Critical significance level	0.05	0.05
	The hypothesis should not be rejected.	
Selected testing method	Chi-square distribution test	
Number of classes used in test	44	44
Significance level	0.29427	0.07958
Critical significance level	0.05	0.05
	The hypothesis should not be rejected.	
Selected testing method	Anderson-Darling test	
Significance level	> 0.15	> 0.15
Critical significance level	0.05	0.05
	The hypothesis should not be rejected.	

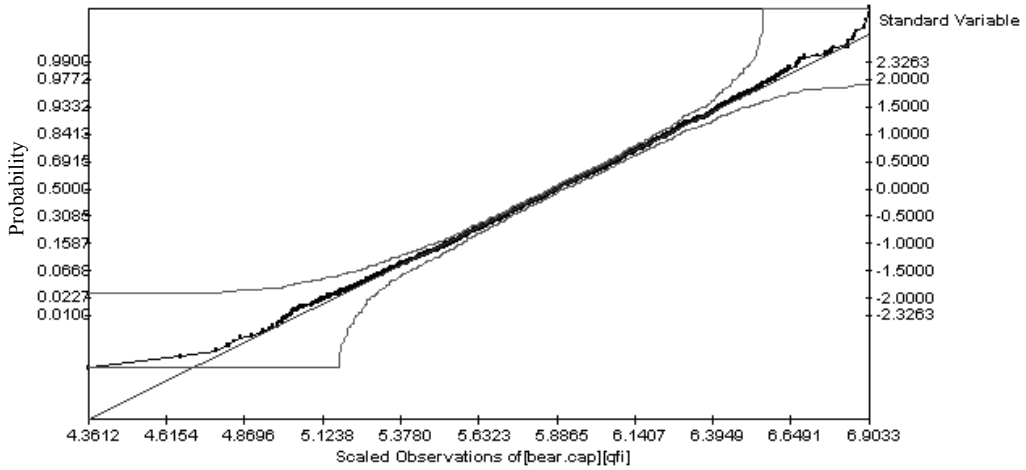

Fig. 12 Lognormal probability chart corresponding to the dataset of bearing capacity in Tables 5 and 6

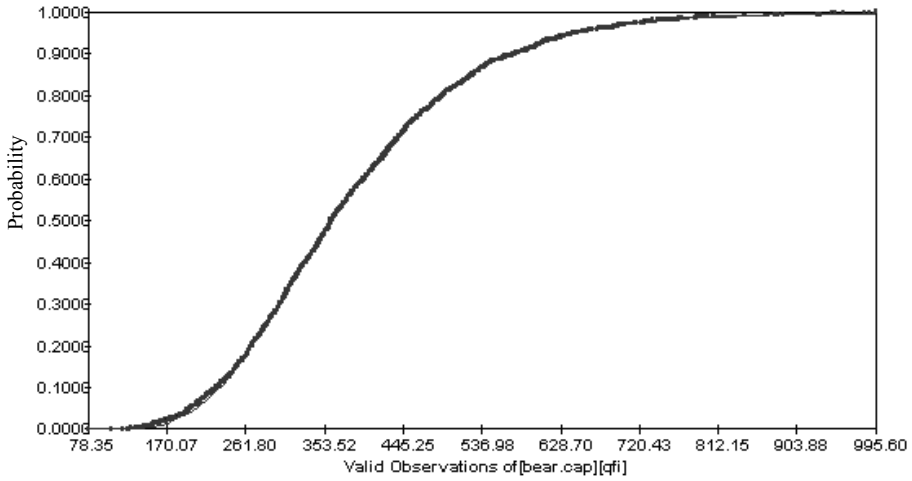

Fig. 13 Lognormal cumulative distribution function of the dataset of bearing capacity in Tables 5 and 6

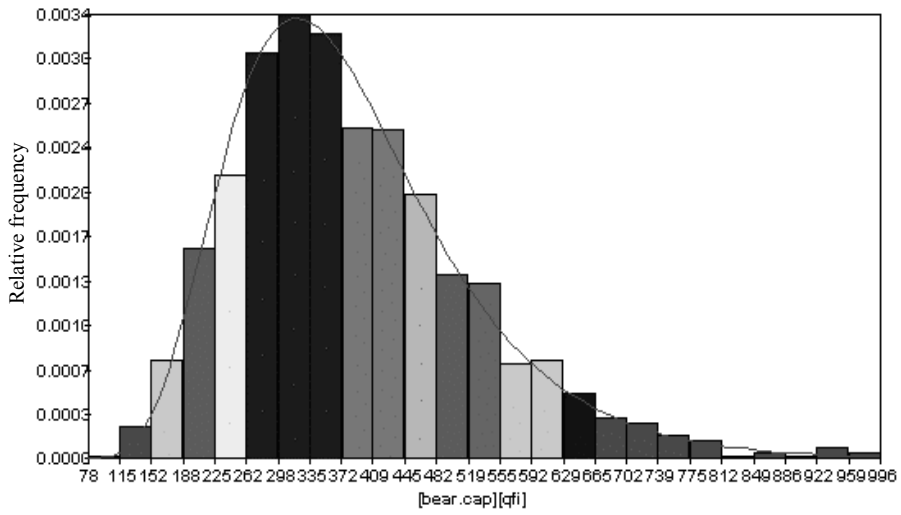

Fig. 14 Lognormal density probability distribution of the dataset of bearing capacity in Tables 5 and 6

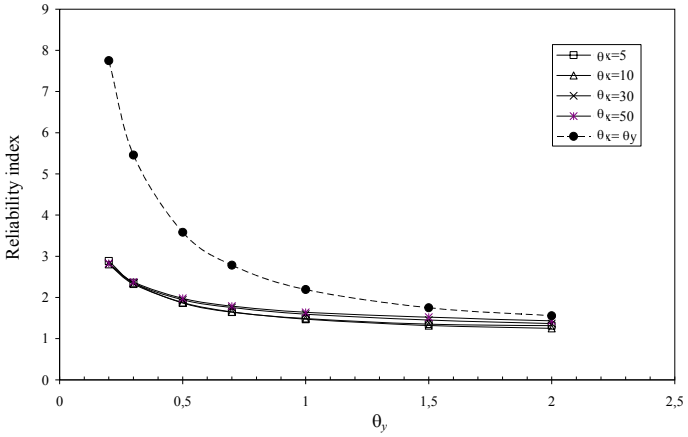

Fig. 15 Reliability index versus vertical scale of fluctuation

6. CONCLUDING REMARKS

The RFEM method has been implemented for geotechnical designing by taking into account the stochastic random fields of soil parameter by local average method. Such method estimates the bearing capacity mean and standard deviation values for calculating reliability index values according to the reliability-based design method suggested by Eurocode 7. The study carried out clearly shows that RFEM can be directly applied for geotechnical design but, in the case of the bearing capacity calculation, the simplification of isotropic random field cannot be accepted for design purposes. Reliable information about coefficient of variation and correlation length of the soil parameters are thus needed for bearing capacity predictions in design practice.

APPENDIX 1

In order to evaluate the influence of the mesh size on the mean value of the bearing capacity simulations with different numbers of elements in the *x* and *y*-directions have been carried out. Figure 16 presents the bearing capacity average versus the number of elements in x direction.

As for computations, 20 elements in *y*-direction have been incorporated for a number of elements less or equal to 50 in *x*-direction, while for a number of elements above 50 (in *x*-direction) 30 elements in *y*-direction have been applied. It can be observed that for a number of element greater than 50 (in *x*-direction) the average of the bearing capacity becomes stable and at 50 reaches its minimal value. Similar effects have been observed in the case in which the number of elements in *y*-direction is changed. The effects are illustrated in Fig. 17.

All computations in this case have been carried out with 50 elements in *x*-direction. The stabilisation begins at 15, but the minimal value is observed at 20. According to what has been demonstrated in this Appendix, the number of realisations in the simulation process is 300. The above results allow to consider the mesh of size 50 × 20, accepted in the paper, as the optimal one.

APPENDIX 2

Since a cross-correlation, usually negative, has been experimentally established for many soil types, the influence of such correlation has been investigated. Namely, the computations have been repeated for three negative correlation coefficients: $\rho = -0.7$, $\rho = -0.5$, $\rho = -0.3$. Examples of results (for the case of correlation lengths θ_x, θ_y) are presented in Fig. 18 (mean values) and Fig. 19 (standard deviations).

It is easy to see that for lack of correlation the average is the lowest and the standard deviation is the greatest. Therefore in the paper the zero-value cross-correlation case has been selected for computational analyses.

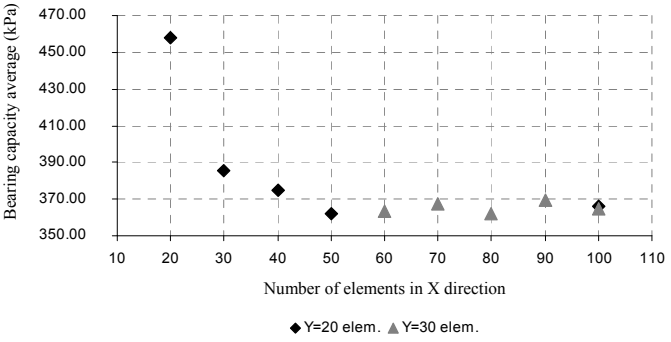

Fig. 16 Bearing capacity average versus number of element in *x*-direction

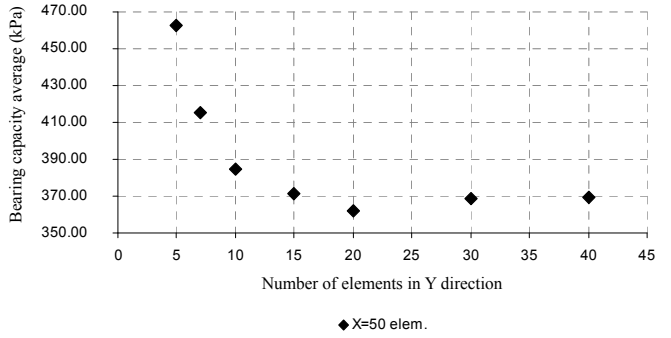

Fig. 17 Bearing capacity average versus number of element in *y*-direction

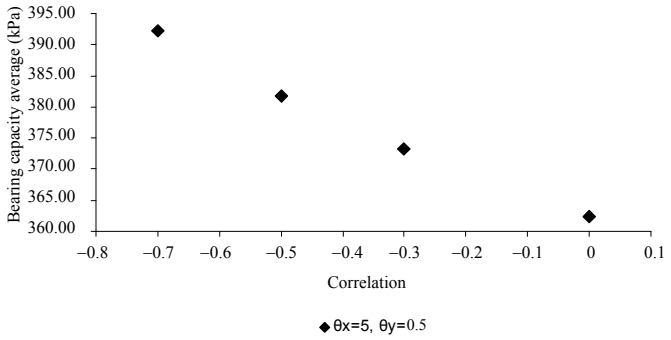

Fig. 18 Bearing capacity averages versus cross-correlation coefficient of strength parameters ϕ and *c*

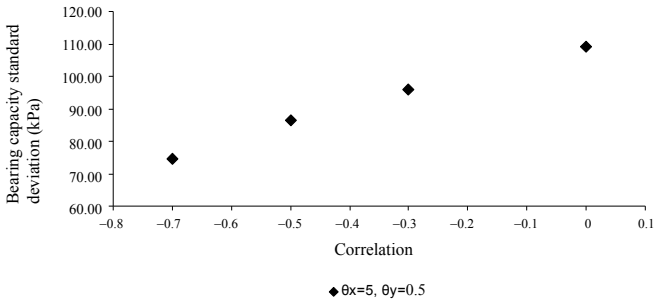

Fig. 19 Bearing capacity standard deviation versus cross-correlation coefficient of strength parameters ϕ and *c*

REFERENCES

Baecher, G. B. and Christian, J. T. (2003). *Reliability and Statistics in Geotechnical Engineering*, Wiley, Chichester, U.K.

Bowles, J. E. (1996). *Foundation Analysis and Design,* 5th Ed., McGrawHill, New York, NY.

Cherubini, C., Vessia, G., and Pula, W. (2007). "Statistical soil characterization of Italian sites for reliability analysis." *Proc. Characterization and Engineering Properties of Natural Soils,* Tan, Phoon, Hight and Lerouell, Eds., Singapore, 2681–2706.

Fenton, G. A. and Vanmarcke, E. H. (1990)."Simulation of random fields via local average subdivision." *Journal of Engineering Mechanics,* ASCE, **116**(8), 1733–1749.

Fenton, G. A. and Griffiths, D. V. (1993). "Statistics of block conductivity through a simple bounded stochastic medium." *Water Resource Res.*, **29**(6), 1825–1830.

Fenton, G. A. and Griffiths, D. V. (2003). "Bearing capacity prediction of spatially random *c* - φ soils." *Canadian Geotechnical Journal*, **40**(1), 54–65.

Fenton, G. A. and Griffiths, D. V. (2005). "Three-dimensional probabilistic foundation settlement." *Journal of Geotechnical and Geoenvironmental Engineering*, **131**(2), 232–239.

Griffiths, D. V. and Fenton, G. A. (1993). "Seepage beneath water retaining structures founded on spatially random soil." *Geotechnique*, **43**(4), 577–587.

Griffiths, D. V. and Fenton, G. A. (2001). "Bearing capacity of spatially random soil: The undrained clay prandtl problem revisited." *Geotechnique*, **54**(4), 351–359.

Griffiths, D. V., Fenton, G. A., and Lemons, C. B. (2002). "Probabilistic analysis of underground pillar stability." *International Journal for Numerical and Analytical Methods in Geomechanics*, **26**, 775–791.

Griffiths, D. V. and Fenton, G. A. (2004). "Probabilistic slope stability by finite elements." *Journal of Geotechnical and Geoenvironmental Engineering*, **130**(5), 507–518.

Griffiths, D. V., Fenton, G. A., and Manoharan, N. (2006). "Undrained bearing capacity of two strip footings on spatially rando soil." *International Journal of Geomechanics*, **6**(6), 421–427.

Puła, W. and Shahrour, I. (2003). "Influence of vertical and horizontal variability of soil strength on the reliability of shallow foundations." *Proc. Symposium International sur les Fondations Superficielles (FONDSUP 2003)*, Paris, **1**, 423–432.

Puła, W. (2004). *Zastosowania Teorii Niezawodności Konstrukcji Do Oceny Bezpieczeństwa Fundamentów*. Oficyna Wydawnicza Politechniki Wrocławskiej.

Robertson, P. K. and Fear, C. E. (1995). "Liquefaction of sands and its evaluation." *Proc. 1st International Conference on Earthquake Geotechnical Engineering*, Keynote Lecture.

Smith, I. M. and Griffiths, D. V. (1998). *Programming the Finite Element Method,* 3rd Ed., John Wiley and Sons, New York, NY.

Terzaghi, K. (1943). *Theoretical Soil Mechanics*, John Wiley and Sons, New York, NY.

Vanmarcke, E. (1984). *Random Fields: Analysis and Synthesis*, MIT Press, Cambridge, MA.

Wickremesinghe, D. and Campanella, R. G. (1991). "Statistical methods for soil layer boundary location using the cone penetration test." *Proc. ICASP6,* Mexico City, **2**, 636–643.